Pertanika J. Sci. & Technol. 24 (2): 423 - 438 (2016)

SCIENCE & TECHNOLOGY

Journal homepage: http://www.pertanika.upm.edu.my/

The Heat Transfer Performance of Gold/Water Nanofluid Flows in Minitube using Thermal Lattice Boltzmann Method

Ahmed A. Hussien[1]*, Mohd Z. Abdullah[2], Mohd A. Al-Nimr[3], N. M. Yusop[1], C. Nuntadusit[4] and M. H. Elnaggar[5]

[1]School of Mechanical Engineering, Engineering Campus, Universiti Sains Malaysia, 14300 Nibong Tebal, Penang, Malaysia

[2]School of Aerospace Engineering, Engineering Campus, Universiti Sains Malaysia, 14300 Nibong Tebal, Penang, Malaysia

[3]Department of Mechanical Engineering, Jordan University of Science and Technology, Irbid 22110, Jordan

[4]Department of Mechanical Engineering, Faculty of Engineering, Prince of Songkla University, HatYai, Songkla, Thailand 90112

[5]Engineering Department Palestine Technical College-Deir EL-Balah Gaza Strip, Palestine

ABSTRACT

One of the best ways to enhance heat transfer coefficient is by improving thermal properties of the working fluid. Gold/water nanofluid flow through horizontal minitube with very low Reynolds number was simulated by using Thermal Lattice Boltzmann Method (TLBM) under uniform heat flux boundary condition. The effect of different volume fraction of nanoparticles on the heat transfer coefficient was studied and compared with the base fluid (water). The results were verified using Finite Volume Method (FVM). The results showed enhancement of heat transfer coefficient when using gold/water nanofluid and this enhancement depends on the volume concentration of Gold nanoparticles. The maximum enhancement was 18% with 0.03 volume concentration.

Keywords: Convective heat transfer, Gold nanoparticles, Nanofluids, TLBM, Axisymmetric, Laminar flow

Article history:
Received: 17 February 2016
Accepted: 22 April 2016

E-mail addresses:
ahmed.a.a.hussien@gmail.com (Ahmed A. Hussien),
mezul@eng.usm.my (Mohd Z. Abdullah),
malnimr@just.edu.jo (Mohd A. Al-Nimr),
menadiah@eng.usm.my (N. M. Yusop),
chayut@me.psu.ac.th (C. Nuntadusit),
mohdhn@yahoo.com (M. H. Elnaggar)
*Corresponding Author

ISSN: 0128-7680

INTRODUCTION

Nowadays, conventional fluid with the addition of ultrafine particles in nanometer size makes a difference in enhancing heat transfer exchange in many applications which emit high heat flux, such as MEMS/NEMS systems, high performance electronic device,

solar cells and many applications that need high performance cooling systems (Hussien et al., 2016; Verma & Tiwari, 2015) . These nanoparticles have thermal conductivity of a hundred times more than conventional fluid. This means that the thermal and rheological properties will be changed upon the addition of nanoparticles to the fluid even at a very low amount (*Zhou* et al., 2012). Moreover, the change depends on the size, shape and the material of the nanoparticles (Anoop et al., 2009; Ji et al., 2011) . Many experimental research have been conducted to identify the physical properties of nanofluids and compared with existing models as described in nanofluids cases (Mostafizur et al., 2015; Solangi et al., 2015) . Besides that, the nanoparticles are continuously in the stage of development by introducing new materials (hybrid nanoparticles), shapes and sizes (Sarkar et al., 2015; Tian et al., 2015) .

So far, the literature survey conducted by researchers have created roles for very small channels to increase the heat transfer coefficient. It is desirable for high heat transfer rate and that is the reason why the contact surface area is higher out of the volume.

Many experimental investigations performed so far have concerned mainly with the study of nanofluids with micro/minichannels for developing a new generation of cooling systems. For instance, Jung et al. (2009) found enhancing the heat transfer up to 30% in their experimental study of AL_2O_3/water nanofluid in rectangle microchannels. Meanwhile, Nitiapiruk et al. (2013) studied TiO_2/water nanofluids in rectangle microchannels experimentally and their results showed that enhancing heat transfer coefficient depends on the volume concentration of the nanoparticles. Nazari et al. (2014) experimented with the performance of the CPU cooling performance by using nanofluids. They used two types of nanoparticles (Al_2O_3 and CNT) dispersant in (water and EG) with various particle concentrations in their experiment. Their results showed 13% maximum enhancement in convection heat transfer which occurred when they used CNT nanoparticles. They also concluded that the maximum enhancement can be achieved when the optimum concentration of nanoparticles and flow rate is taken into consideration.

Recently, numerical simulations of testing the enhancement of heat transfer performance when using nanofluids in micro/minichannels were taken into account for avoiding experimental fabrication efforts and saving time and money. Jang and Choi (2006) investigated numerically Cu/water and diamond/water nanofluids in rectangle microchannels heat sink. The enhancement in thermal performance was about 10%. In another study, J. Li and Kleinstreuer (2008) worked numerically to find out CuO/water nanofluid in trapezoidal microchannels leading to extra pressure drop with the enhancement of heat transfer. Mohammed et al. (2011) tested six different types of nanofluids (Al_2O_3, Ag, CuO, diamond, SiO_2 and TiO_2)/water in triangular microchannels numerically and based on their observation, the peak thermal performance and less pressure drop can be utilised using Diamond and Ag /water nanofluids. Salman et al. (2012) studied convection heat transfer of (Al_2O_3, CuO,SiO_2, ZnO) / EG nanofluids flow through circular microchannel with different nanoparticle sizes and volume concentrations. Their results revealed significant effects on the Nusselt number, velocity, wall shear stress and pressure drop with the change of size and concentration of the nanoparticles. Mohammadian et al. (2014) studied the performance of counter flow microchannel heat exchanger when using Al_2O_3–water nanofluid numerically. They used different nanoparticle volume concentrations

and sizes. The results pinned that the highest thermal performance can be achieved using the highest concentration and the smallest particle size.

Some researchers prefer the minichannel when using nanofluids by for two main reasons: the cost of fabrication and less of pressure drop (Shenoy et al., 2011). Ijam and Saidur (2012) studied the cooling performance of the heat sink by using the SiC–water and TiO_2– water in the minichannel. They found out that the improvement was between 7–12%. Liu and Yu (2011) investigated experimentally convective heat transfer Al_2O_3/water nanofluid flow inside circular minichannel (Di= 1.09 mm) in different flow types of laminar and transition and turbulence. Their results revealed that the laminar flow caused greater enhancement compared with the transition and turbulent flow with pressure drop penalty while the conventional correlations can be used in the laminar regime. Vafaei and Wen (2012) studied the Al_2O_3/water nanofluid flow inside circular minichannel (Di= 510 μm). The enhancement of the heat transfer coefficient reached 40% for higher flow rate. In addition, Al_2O_3/water nanofluid with rectangle minichannels heat sink was investigated experimentally by Ho et al. (2014) with the hydraulic diameter at 1.2 mm. Ijam et al. (2012) investigated (Al2O3, TiO2)/water nanofluids flow through rectangle minichannels heat sink. Hassan et al. (2013) concluded that nanofluids with laminar flow in minichannels are a superior coolant when compared between the circular minichannel (Di=3mm) and microchannel (Di=50 μm) with Al_2O_3/water nanofluid.

Many types of nanofluids have been studied so far for high thermal conductivity of metal nanoparticles, such as Au, Ag, Cu, Al, which made it highly demanding for being the perfect coolant in the recent market. However, very few researches have been concerned with the convection of heat transfer performance on gold/water nanofluid. Sabir et al. (2015) studied experimentally the characteristics of convection heat transfer of gold nanofluid with very low volume concentrations and their results detected up to 30% of enhancement in heat transfer coefficient. On the other hand, Patel et al. (2003) detected 9% thermal conductivity enhancement in their experimental research when they used Au/water nanofluid, while Tsai et al. (2004) revealed that using gold/water nanofluid reduced the thermal resistance of the heat pipes.

In the past few years, researchers have started using the **Thermal Lattice Boltzman Method** (TLBM), which is considered as a very effective method to simulate many problems for fluid and thermal flow (Sidik & Razali, 2014). Sheikholeslami et al. (2013) applied TLBM to figure the magnetic field effect to concentric annuals filled by A_2O_3/H_2O nanofluid. In another research, Karimipour et al. (2015) used TLBM the force convection of Cu/H_2O nanofluid flow inside the microtube in very low Reynolds number with slip wall flow boundary condition.

This article focuses on the enhancement of heat transfer coefficient by using gold/water nanofluid flow inside the minitube with different volume concentrations using TLBM.

GEOMETRY MODELING AND GOVERNING EQUATIONS

The continuity, 2-D Navier-Stokes and energy equations will be used to describe the flow velocities and temperature distributions in the whole region. Figure 1 shows the computational domain, the axial and radial axis (z, r) respectively, and the uniform heat flux (q") which will be exposed to the outer surface of the minitube. According to Kandlinkar classifications

(Kandlikar, 2006), the channel that has hydraulic diameter from 200μm to 3mm is considered minichannel, whereas the minitube diameter is 2.1 mm with wall thickness of 0.45 mm.

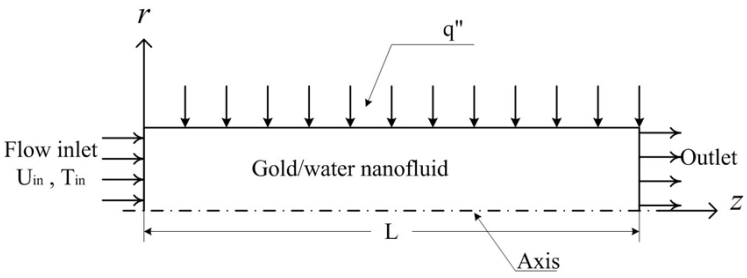

Figure 1. Schematic diagram

The governing equations are:

$$\frac{1}{r}\frac{\partial}{\partial r}(vr)+\frac{\partial u}{\partial z}=0 \quad [1]$$

$$u\frac{\partial u}{\partial z}+v\frac{\partial u}{\partial r}=-\frac{1}{\rho}\frac{\partial p}{\partial z}+\vartheta\left(\frac{\partial^2 u}{\partial z^2}+\frac{\partial^2 u}{\partial r^2}+\frac{1}{r}\frac{\partial u}{\partial r}\right) \quad [2]$$

$$u\frac{\partial v}{\partial z}+v\frac{\partial v}{\partial r}=-\frac{1}{\rho}\frac{\partial p}{\partial r}+\vartheta\left(\frac{\partial^2 v}{\partial z^2}+\frac{\partial^2 v}{\partial r^2}+\frac{1}{r}\frac{\partial v}{\partial r}-\frac{v}{r^2}\right) \quad [3]$$

$$u\frac{\partial T}{\partial z}+v\frac{\partial T}{\partial r}=\frac{\vartheta}{P_r}\left(\frac{\partial^2 T}{\partial z^2}+\frac{\partial^2 T}{\partial r^2}+\frac{1}{r}\frac{\partial T}{\partial r}\right) \quad [4]$$

where u, v are the velocity components in z and r directions respectively.

The following assumptions will be considered:

- Continuum.
- Newtonian fluid.
- Incompressible.
- Constant viscosity, density, and thermal conductivity.
- Negligible gravity force.
- Negligible nuclear, electromagnetic and radiation energy transfer

NUMERICAL METHOD

Nanofluids Treatment

In this paper, we used gold-water nanofluid as homogenous working fluid. The physical and thermal properties of the nanofluid were calculated from the properties of water and gold as shown in Table 1.

Table 1
The Properties of Water and Gold nanoparticles at T=313.15K (Bergman et al., 2011)

	ρ (kg m^{-3})	C_p (J kg^{-1} K^{-1})	μ (kg m^{-1} s^{-1})	K (W m^{-1} K^{-1})
Water	992.22	4178	0.0006532	0.6305
Gold nanoparticles	19300	126	-	318

The general formulas for fluid-solid mixture was used to find the density and specific heat capacity of the nanofluids:

$$\rho_{nf} = (1-\varphi)\rho_f + \varphi\rho_p \quad [5]$$

$$(c_p\rho)_{nf} = (1-\varphi)(c_p\rho)_f + \varphi(c_p\rho)_p \quad [6]$$

Batchelor's model (Batchelor, 1977) was used to calculate the effective viscosity of nanofluids:

$$\mu_{eff} = (1+2.5\phi+6.2\phi^2)\mu_{bf} \quad [7]$$

The effective thermal conductivity was calculated by using the Hamilton and crosser model (Hamilton & Crosser, 1962):

$$k_{eff} = k_{bf}\frac{k_p+(n-1)k_{bf}+(n-1)(k_p-k_{bf})\phi}{k_p+(n-1)k_{bf}-(k_p-k_{bf})\phi} \quad [8]$$

where the kinematic viscosity is $v = \mu/\rho$, the prandtl number is $P_r = c_p\mu/k$ and the thermal diffusivity is $\alpha = v/P_r$.

According to Hamilton and Crosser (1962), increasing the volume concentration caused an increase in the thermal conductivity and the viscosity in the crosser model and Batchelor's model, as can be seen in Figure 2.

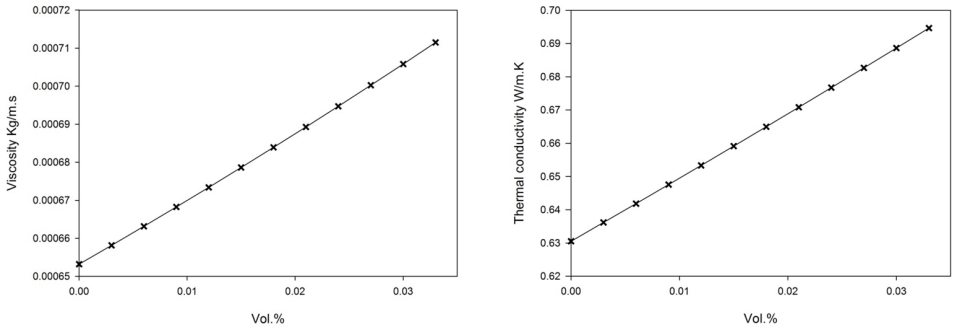

(a) (b)

Figure 2. The effect of the nanoparticles volume concentrations on the (a) viscosity and (b) thermal conductivity

Lattice Boltzmann Methods

Numerical simulations are considered over experimental at the situations where it becomes tedious to collect data from setup. Numerical methods are preferable because experimental setup needs very high treatment care, special tools and expensive instruments. Thus, the Thermal Lattice Boltzman Method (TLBM) has become a very significant research technique in mini/ microchannels with nanofluids (Yang & Lai, 2011). In this study, TLBM was used for the analysis of fluid flow and heat transfer in minitube, with uniform heat flux.

The idea of Lattice Boltzmann Method (LBM) is to take advantage of micro-scale and macro-scale by considering a collection of particles as a unit, which is called the meso-scale. For instance, LBM is connected between the entropy of a system with time and the change in macroscopic variables. It can predict the macroscopic behaviour by studying the distribution functions which is in a general probability of finding particles in Lattice Unite at a certain time f(r,c,t) and g(r,c,t) respectively.

Halliday et al. (2001) were the first to explore the energy equation in axisymmetry by LGK approximation with selected source terms. Later, many models studied the axisymmetric flow such as those by Lee et al. (2006), Reis and Phillips (2008), Guo et al. (2009) and J. G. Zhou (2011).

In this paper, Zhou's model (J. G. Zhou, 2011) was used to define the source terms in the D2Q9 LB Model, the distribution function of nine velocities were formulated as:

$$f_\alpha(\boldsymbol{x}+e_\alpha\Delta t,t+\Delta t)=\omega_\alpha f_\alpha^{eq}(\boldsymbol{x},t)+(1-\omega_\alpha)f_\alpha(\boldsymbol{x},t)+w_\alpha\theta\Delta t+\frac{\Delta t}{\forall e^2}e_{\alpha i}F_i \quad [9]$$

the source terms θ and F_i are defined as: $\theta=\frac{-\rho u_r}{r}$, and $F_i=\frac{-\rho u_i u_r}{r}-\frac{2\rho\nu u_i}{r}\delta_{ir}$ respectively. where f_α is the distribution functions, $\boldsymbol{x}$ is the position vector $\boldsymbol{x}=\boldsymbol{x}(z,r)$, ω_α the effective relaxation time depends on the position, *i* index represents *z* and *r*. The other parameters of the D2Q9 model are shown in Table 2.

Table 2
D2Q9 LBM Model Variables (Mohamad, 2011)

C_s^2	A	$e_{\alpha i}$	w_α
	0	(0,0)	4/9
1/3	1,2,3,4	$(\cos\frac{\alpha-1}{2}\pi,\sin\frac{\alpha-1}{2}\pi)$	1/9
	5,6,7,8	$\sqrt{2}(\cos(\frac{\alpha-5}{2}\pi+\frac{\pi}{4}),\sin(\frac{\alpha-5}{2}\pi+\frac{\pi}{4}))$	1/36

The equilibrium distribution function can be formulated as:

$$f_\alpha^{eq}=w_\alpha\rho\left(1+\frac{e_{\alpha i}\mathbf{u}_i}{C_s^2}+\frac{1}{2}\frac{e_{\alpha i}e_{\alpha j}\mathbf{u}_i\mathbf{u}_j}{C_s^4}+\frac{1}{2}\frac{\mathbf{u}_i\mathbf{u}_j}{C_s^2}\right) \quad [10]$$

The distribution functions give the density and the velocity as:

$$\rho(\boldsymbol{x}, t) = \sum_{\alpha} f_{\alpha}(\boldsymbol{x}, t) \quad [11]$$

$$\mathbf{u}_{\mathrm{i}} = \frac{1}{\rho}\sum_{\alpha} \mathrm{e}_{\alpha \mathrm{i}} f_{\alpha}(\boldsymbol{x}, t) \quad [12]$$

Peng et al. (2003) proposed the first axisymmetric flow in TLBM by solving the temperature distribution with finite difference method. The hybrid model was then used to solve the thermal and vorticity stream function (Sheng Chen et al., 2009).

In recent times, the dual lattice form has been used to recover thermal energy equation by new distribution function g(x,t) with f(x,t) (Wang et al., 2007; Q. Li et al., 2009; Zheng et al., 2010). In this paper, D2Q4 thermal model was used for solving the temperature distributions, which in turn helps to reduce the computational efforts over D2Q9 thermal model (Djebali et al., 2008). In this model, the scalar distribution function can be derived from the following formulation:

$$g_{\gamma}\left(\boldsymbol{x} + e_{\gamma}\Delta t, t + \Delta t\right) = \omega_{\gamma} g_{\gamma}^{eq}(\boldsymbol{x}, t) + \left(1 - \omega_{\gamma}\right) g_{\gamma}(\boldsymbol{x}, t) + w_{\gamma}\Delta t\ (1 + 0.5\omega_{\gamma}) \quad [13]$$

where:

$S = \frac{\alpha}{r}\frac{\partial T}{\partial r}$, $\omega_{\gamma} = \frac{1}{\tau_g}$ and the relation between thermal diffusivity $\boldsymbol{\alpha}$ and thermal relaxation time τ_g is $\boldsymbol{\alpha} = \frac{\tau_g - 0.5}{\mathbf{2}}\frac{\Delta \boldsymbol{x}^{\mathbf{2}}}{\Delta \boldsymbol{t}}$. The equilibrium distribution $\mathrm{g}_{\gamma}^{\mathrm{eq}}(\mathrm{x}, \mathrm{t}) = \mathrm{w}_{\gamma}\mathrm{T}\left(1 + \frac{\mathrm{e}_{\gamma \mathrm{i}}\mathrm{u}_{\mathrm{i}}}{\mathrm{C}_{\mathrm{s}}^{2}}\right)$, where $\mathrm{C}_{\mathrm{s}}^{2} = \frac{1}{2}$, $\mathrm{w}_{\gamma 1-4} = \frac{1}{4}$ and $\mathrm{e}_{\gamma \mathrm{i}}$ as shown in Fig. 3.

The macroscopic temperature is obtained similarly as that of flow distribution functions:

$$\mathrm{T} = \sum_{\gamma} \mathrm{g} + \frac{\Delta \mathrm{t}}{2}\mathrm{S} \quad [14]$$

Boundary conditions

After the streaming process, f_1, f_5, f_8 *and* g_1 are unknown at the inlet and for outlet its f_3, f_6, f_7 *and* g_2. N`ow at the wall, f_4, f_8, f_7 *and* g_4 and at the axis f_2, f_5, f_6 *and* g_{12} as shown in Figure 3.

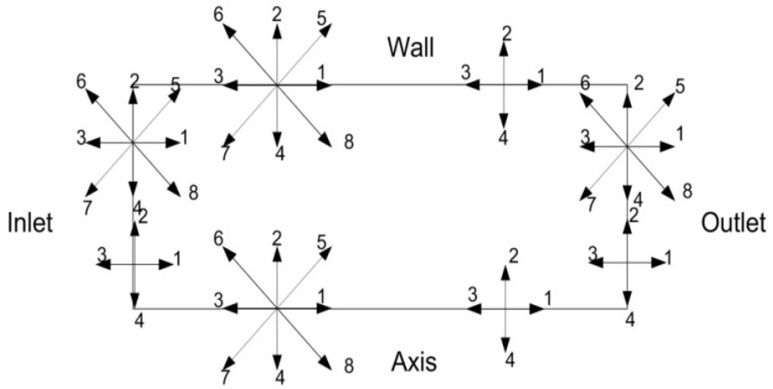

Figure 3. Distribution functions at the boundaries for D2Q9-D2Q4 flow thermal model

Applying boundary conditions helps to locate the unknown distribution functions. For a boundary condition with nonzero velocity, the inlet flow in the west side is known, so the bounce-back scheme is obviously invalid. The Zou and He (Zou & He, 1997) boundary condition for known inlet velocity was used, whereas for constant inlet temperature, $\mathbf{T_0}$ was divided to scalar distribution function and hence, the macroscopic and microscopic boundary conditions are:

$$z = 0 \begin{cases} u_z = U_0 \\ u_r = 0.0 \\ T_i = T_0 \end{cases} \rightarrow \begin{cases} \rho_w = \frac{1}{1-U_0}[f_0 + f_2 + f_4 + 2(f_3 + f_6 + f_7)] \\ f_1 = f_3 + \frac{2}{3}\rho_w U_0 \\ f_5 = f_7 - \frac{1}{2}(f_2 - f_4) + \frac{1}{6}\rho_w U_0 \\ f_8 = f_6 - \frac{1}{2}(f_2 - f_4) + \frac{1}{6}\rho_w U_0 \\ g_1 = (w_1 + w_3)T_0 - g_3 \end{cases} \quad [15]$$

For constant heat flux at the wall, the bounce back boundary (Shiyi Chen et al., 1996) condition was used to the flow distribution function, and constant temperature gradient for scalar distribution functions is expressed as (Tarokh et al., 2013):

$$r = R \begin{cases} u_r = 0.0 \\ u_z = 0.0 \\ -k\frac{\partial T}{\partial r} = q_0^{"} \end{cases} \rightarrow \begin{cases} f_4 = f_2 \\ f_7 = f_5 \\ f_8 = f_6 \\ g_4 = (w_2 + w_4)\frac{q_0^{"}}{k} - g_2 + \sum_1^4 g \end{cases} \quad [16]$$

Simple forward finite's difference scheme was used to define the unknown distribution function around the central axis as shown in Eq. (17).

$$r = 0 \begin{cases} \frac{\partial u}{\partial r} = 0 \\ \frac{\partial T}{\partial r} = 0 \end{cases} \longrightarrow \begin{cases} f^1_{\alpha=0-9} = f^2_{\alpha=0-9} \\ g^1_{\gamma=1-4} = g^2_{\gamma=1-4} \end{cases} \quad [17]$$

As outlet density and velocity are unknown, it is assumed that velocity at the point before last lattice is the outlet velocity and the same procedure of inlet boundary condition is applied (Mohamad, 2011). For thermal distribution function, the extrapolation was used to define the unknown value.

Figure 4 shows the sequence steps for each time step to solve BKG-LBM D2Q9-D2Q4 flow thermal models until convergence (Mohamad, 2011).

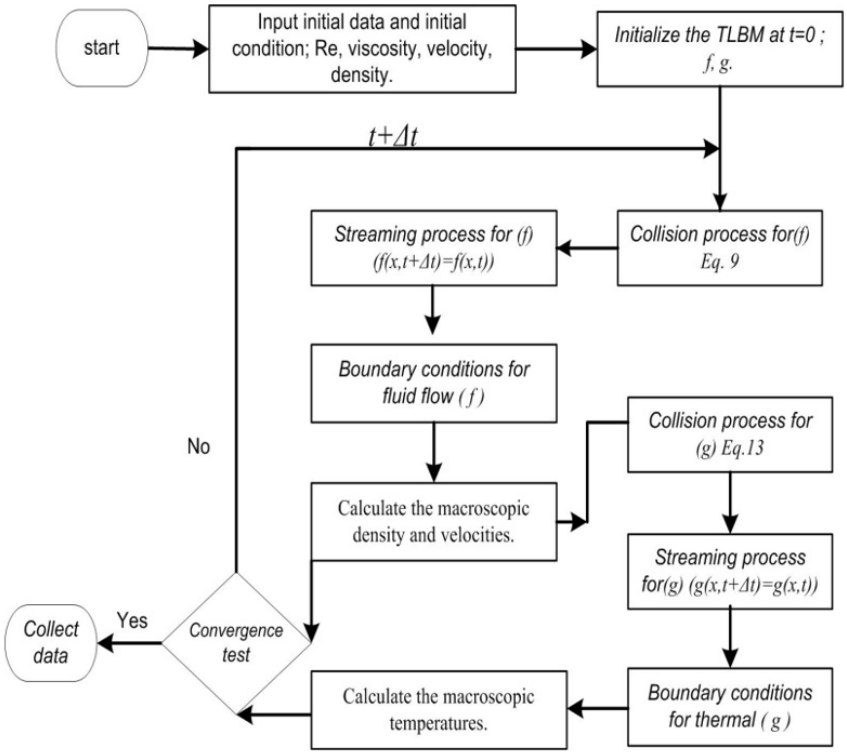

Figure 4. The TLBM steps

DISCUSSION

In this simulation, the uniform heat flux was applied at the surface of the tube $q''_0 = 6000\ {}^{W}/_{m^2}$, with low Reynolds number $(\mathrm{Re} = 50)$ for all process fluids. In total, four different volume concentrations of gold nanoparticles were used to perform the experiment, namely 0.1,0.5,1 and 3% volume concentrations. The enhancement of heat transfer coefficient through axial distance was studied by using a 2.1 mm diameter minitube and 27cm axial length.

Thus, the local heat transfer coefficient was calculated by applying the Newton law:

$$h(z) = \frac{q_0^{"}}{(T_w(z) - T_m(z))} \quad [18]$$

where T_{wi} is the temperature of the inner wall surface and $T_m(z)$ is the mean temperature in the z location and can be predicted by using the following formulae:

$$T_m(z) = \frac{\int_0^R \rho u T \, dr}{\rho_m u_m} \quad [19]$$

ρ_m , u_m is the mean density and the mean axial velocity in the same axial point respectively:

$$\theta(z, r) = \frac{T(z,r) - T_m(z)}{q^{"} l / k} \quad [20]$$

The results of D2Q9-D2Q4 TLBM showed acceptable values as compared with commercial CFD package. From Figure 5 and Figure 6, it can be easily confirmed that wall temperature along the axial direction and cross section temperature distribution in different axial locations are almost matching respectively.

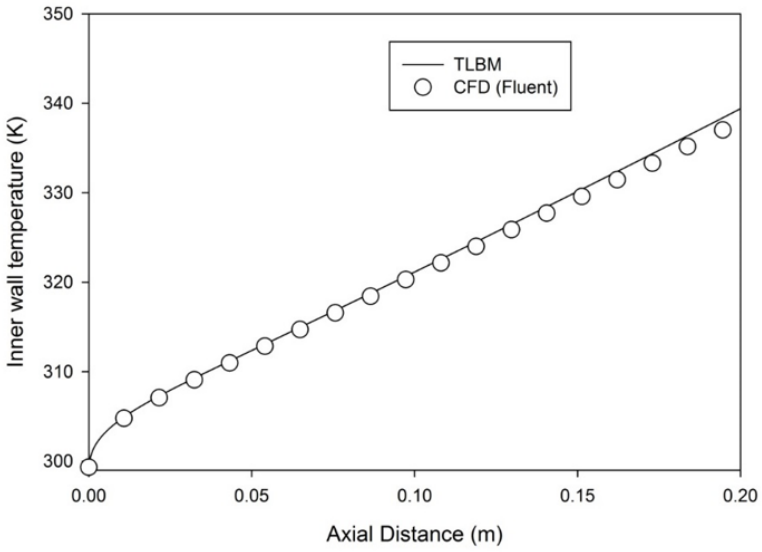

Figure 5. The Inner wall temperature along the axial direction for water

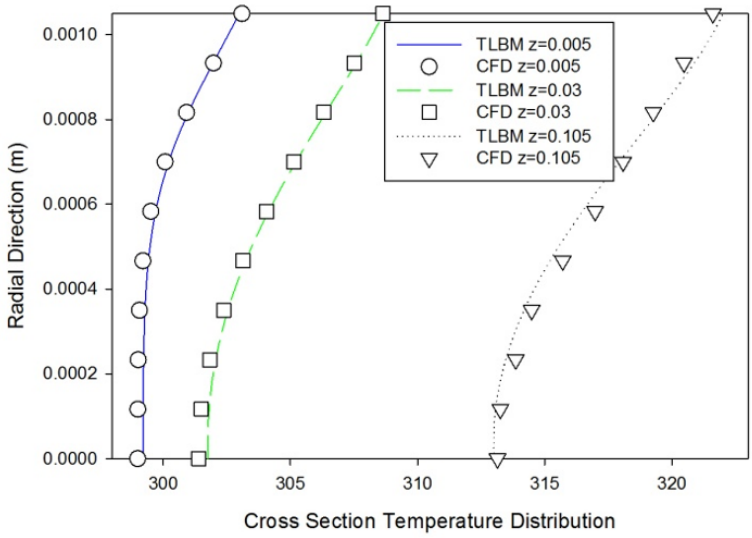

Figure 6. Temperature distribution for different axial locations

Figure 7 shows the dimensionless inner wall temperature $\theta_{w,}$ with reference to Eq.20 along the axial distance ranges from 0 - 0.27m. This curve indicates that the increase in volume concentration of nanoparticles will decrease the dimensionless wall temperature. This is due to the increase in effective thermal conductivity of the nanofluids, which in turn improves the heat transfer along the radial direction. This relation can be seen especially in the fully developed regions.

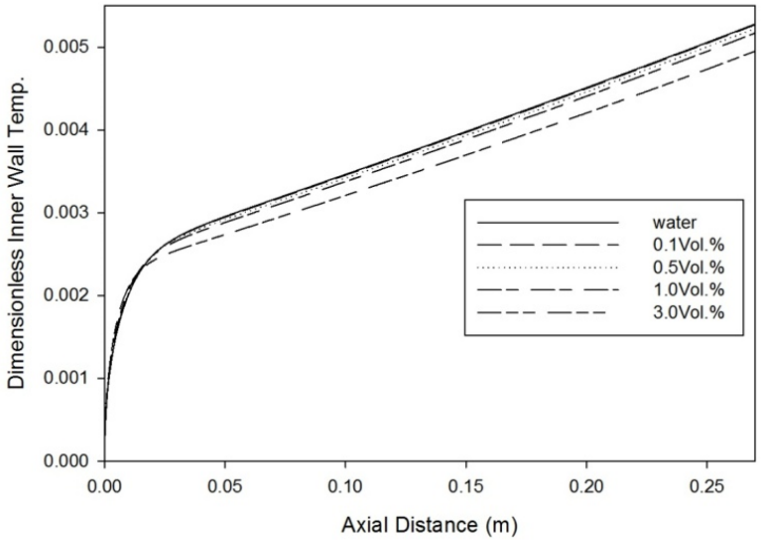

Figure 7. The dimensionless inner wall temperature variation with different nanoparticles volume concentration

Figure 8 shows heat transfer coefficient along axial direction by considering volume concentrations of gold nanoparticles. It can be seen that heat transfer coefficient increases with the increase in concentration of the gold/water nanofluid. Now comparing results with that of water, we found out that there is an enhancement of 18% for 3.0vol.% gold/water nanofluid. Hence, for very low concentration of 0.1vol.%, the enhancement was around 1%. With these figures, a much large enhancement was seen at the beginning of the developing region.

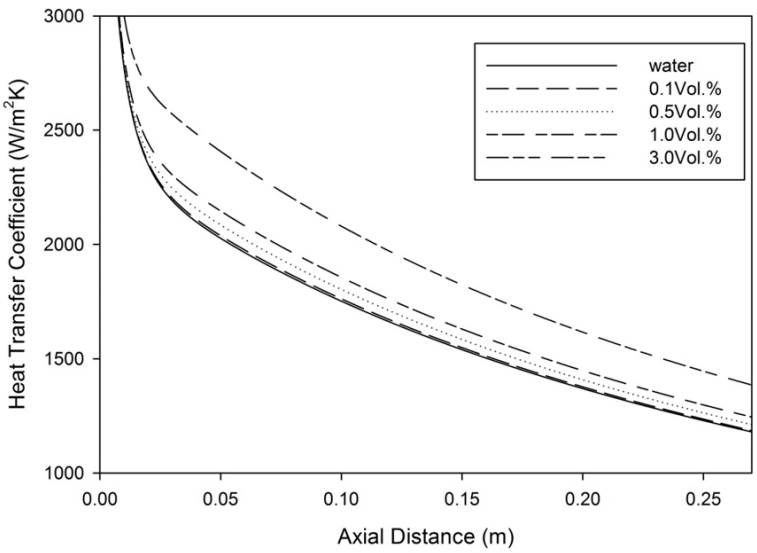

Figure 8. The heat transfer coefficient variation with different volume concentrations of nanoparticles

The average Nusselt number increases with the increase in volume concentration of gold nanoparticle, as shown in Figure 9. The results show very low enhancement in average Nusselt number which is due to the enhancing of nanofluids thermal conductivity. The maximum developing value of Average Nusselt number in comparing water is 7% for 3.0vol.% gold/water nanofluid.

The major advantage of using nanofluids will not only boost effective thermal conductivity but also drastically enhance viscosity. For example, the velocity of the 3.0vol.% gold/water nanofluid is about 30% less than the velocity of water at the same Reynolds number. This shows that the reduction in the mean velocity causes more heat carrier.

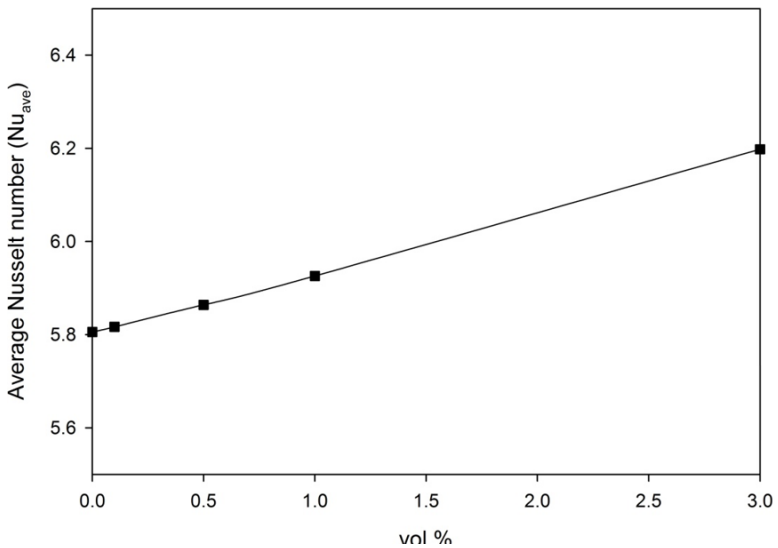

Figure 9. Average Nusselt number variation with different volume concentrations of nanoparticles

Nowadays, research on gold/water nanofluid is rarely seen, thus more experimental research must be carried out in this area for a comprehensive understanding.

CONCLUSION

The Thermal Lattice Boltzmann Method (D2Q9-D2Q4 TLBM) has been used to simulate the force convection heat transfer by using gold/water nanofluid with different volume concentrations through minitube. The results pinned that heat transfer coefficient enhances with gold/water nanofluid over pure water. Furthermore, the enhancement depends on the volume concentration of the gold nanoparticles proportionally. From this study, the maximum enhancement was 20% for 0.03 volume concentration of gold/water nanofluid compared with water. The enhancement of the heat transfer coefficient was due to the effective thermal conductivity and effective viscosity. From this study, it has been observed that there is a shortage in the investigation of gold/water nanofluid and its effects in enhancing heat transfer coefficient experimentally.

ACKNOWLEDGEMENTS

The first author would like to thank Universiti Sains Malaysia (USM) for the financial support provided for a PhD student through the USM fellowship.

REFERENCES

Anoop, K., Sundararajan, T., & Das, S. K. (2009). Effect of particle size on the convective heat transfer in nanofluid in the developing region. *International Journal of Heat and Mass Transfer, 52*(9), 2189-2195.

Batchelor, G. (1977). The effect of Brownian motion on the bulk stress in a suspension of spherical particles. *Journal of Fluid Mechanics, 83*(01), 97-117.

Bergman, T. L., Incropera, F. P., & Lavine, A. S. (2011). *Fundamentals of heat and mass transfer*: John Wiley & Sons.

Chen, S., Martinez, D., & Mei, R. (1996). On boundary conditions in lattice Boltzmann methods. *Physics of Fluids (1994-present), 8*(9), 2527-2536.

Chen, S., Tölke, J., & Krafczyk, M. (2009). Simple lattice Boltzmann subgrid-scale model for convectional flows with high Rayleigh numbers within an enclosed circular annular cavity. *Physical Review E, 80*(2), 026702.

Djebali, R., Pateyron, B., El Ganaoui, M., & Sammouda, H. (2008). Axisymmetric high temperature jet behaviours based on a lattice Boltzmann computational method. Part I: Argon Plasma.

Guo, Z., Han, H., Shi, B., & Zheng, C. (2009). Theory of the lattice Boltzmann equation: lattice Boltzmann model for axisymmetric flows. *Physical Review E, 79*(4), 046708.

Halliday, I., Hammond, L., Care, C., Good, K., & Stevens, A. (2001). Lattice Boltzmann equation hydrodynamics. *Physical Review E, 64*(1), 011208.

Hamilton, R., & Crosser, O. (1962). Thermal conductivity of heterogeneous two-component systems. *Industrial and Engineering Chemistry Fundamentals, 1*(3), 187-191.

Hassan, M., Sadri, R., Ahmadi, G., Dahari, M. B., Kazi, S. N., Safaei, M. R., & Sadeghinezhad, E. (2013). Numerical study of entropy generation in a flowing nanofluid used in micro-and minichannels. *Entropy, 15*(1), 144-155.

Ho, C., Chen, W.-C., & Yan, W.-M. (2014). Correlations of heat transfer effectiveness in a minichannel heat sink with water-based suspensions of Al 2 O 3 nanoparticles and/or MEPCM particles. *International Journal of Heat and Mass Transfer, 69*, 293-299.

Hussien, A. A., Abdullah, M. Z., & Moh'd A, A.-N. (2016). Single-phase heat transfer enhancement in micro/minichannels using nanofluids: Theory and applications. *Applied Energy, 164*, 733-755.

Ijam, A., & Saidur, R. (2012). Nanofluid as a coolant for electronic devices (cooling of electronic devices). *Applied Thermal Engineering, 32*, 76-82.

Ijam, A., Saidur, R., & Ganesan, P. (2012). Cooling of minichannel heat sink using nanofluids. *International Communications in Heat and Mass Transfer, 39*(8), 1188-1194.

Jang, S. P., & Choi, S. U. (2006). Cooling performance of a microchannel heat sink with nanofluids. *Applied Thermal Engineering, 26*(17), 2457-2463.

Ji, Y., Wilson, C., Chen, H.-h., & Ma, H. (2011). Particle shape effect on heat transfer performance in an oscillating heat pipe. *Nanoscale Research Letters, 6*(1), 1-7.

Jung, J.-Y., Oh, H.-S., & Kwak, H.-Y. (2009). Forced convective heat transfer of nanofluids in microchannels. *International Journal of Heat and Mass Transfer, 52*(1), 466-472.

Kandlikar, S. G. (2006). Effect of liquid-vapor phase distribution on the heat transfer mechanisms during flow boiling in minichannels and microchannels. *Heat Transfer Engineering, 27*(1), 4-13.

Karimipour, A., Nezhad, A. H., D'Orazio, A., Esfe, M. H., Safaei, M. R., & Shirani, E. (2015). Simulation of copper–water nanofluid in a microchannel in slip flow regime using the lattice Boltzmann method. *European Journal of Mechanics-B/Fluids, 49*, 89-99.

Lee, T., Huang, H., & Shu, C. (2006). An axisymmetric incompressible lattice Boltzmann model for pipe flow. *International Journal of Modern Physics C, 17*(05), 645-661.

Li, J., & Kleinstreuer, C. (2008). Thermal performance of nanofluid flow in microchannels. *International Journal of Heat and Fluid Flow, 29*(4), 1221-1232.

Li, Q., He, Y., Tang, G., & Tao, W. (2009). Lattice Boltzmann model for axisymmetric thermal flows. *Physical Review E, 80*(3), 037702.

Liu, D., & Yu, L. (2011). Single-phase thermal transport of nanofluids in a minichannel. *Journal of Heat Transfer, 133*(3), 031009.

Mohamad, A. A. (2011). *Lattice Boltzmann method: fundamentals and engineering applications with computer codes*: Springer Science & Business Media.

Mohammadian, S. K., Seyf, H. R., & Zhang, Y. (2014). Performance Augmentation and Optimization of Aluminum Oxide-Water Nanofluid Flow in a Two-Fluid Microchannel Heat Exchanger. *Journal of Heat Transfer, 136*(2), 021701.

Mohammed, H., Gunnasegaran, P., & Shuaib, N. (2011). The impact of various nanofluid types on triangular microchannels heat sink cooling performance. *International Communications in Heat and Mass Transfer, 38*(6), 767-773.

Mostafizur, R., Saidur, R., Aziz, A. A., & Bhuiyan, M. (2015). Thermophysical properties of methanol based Al 2 O 3 nanofluids. *International Journal of Heat and Mass Transfer, 85*, 414-419.

Nazari, M., Karami, M., & Ashouri, M. (2014). Comparing the thermal performance of water, Ethylene Glycol, Alumina and CNT nanofluids in CPU cooling: Experimental study. *Experimental Thermal and Fluid Science, 57*, 371-377.

Nitiapiruk, P., Mahian, O., Dalkilic, A. S., & Wongwises, S. (2013). Performance characteristics of a microchannel heat sink using TiO 2/water nanofluid and different thermophysical models. *International Communications in Heat and Mass Transfer, 47*, 98-104.

Patel, H. E., Das, S. K., Sundararajan, T., Nair, A. S., George, B., & Pradeep, T. (2003). Thermal conductivities of naked and monolayer protected metal nanoparticle based nanofluids: Manifestation of anomalous enhancement and chemical effects. *Applied Physics Letters, 83*(14), 2931-2933.

Peng, Y., Shu, C., Chew, Y., & Qiu, J. (2003). Numerical investigation of flows in Czochralski crystal growth by an axisymmetric lattice Boltzmann method. *Journal of Computational Physics, 186*(1), 295-307.

Reis, T., & Phillips, T. N. (2008). Numerical validation of a consistent axisymmetric lattice Boltzmann model. *Physical Review E, 77*(2).

Sabir, R., Ramzan, N., Umer, A., & Muryam, H. (2015). An experimental study of forced convective heat transfer characteristic of gold water nanofluid in laminar flow. *Science International, 27*(1).

Salman, B., Mohammed, H., & Kherbeet, A. S. (2012). Heat transfer enhancement of nanofluids flow in microtube with constant heat flux. *International Communications in Heat and Mass Transfer, 39*(8), 1195-1204.

Sarkar, J., Ghosh, P., & Adil, A. (2015). A review on hybrid nanofluids: Recent research, development and applications. *Renewable and Sustainable Energy Reviews, 43*, 164-177.

Sheikholeslami, M., Gorji-Bandpy, M., & Ganji, D. (2013). Numerical investigation of MHD effects on Al 2 O 3–water nanofluid flow and heat transfer in a semi-annulus enclosure using LBM. *Energy, 60*, 501-510.

Shenoy, S., Tullius, J., & Bayazitoglu, Y. (2011). Minichannels with carbon nanotube structured surfaces for cooling applications. *International Journal of Heat and Mass Transfer, 54*(25), 5379-5385.

Sidik, N. A. C., & Razali, S. A. (2014). Lattice Boltzmann method for convective heat transfer of nanofluids–A review. *Renewable and Sustainable Energy Reviews, 38*, 864-875.

Solangi, K. H., Kazi, S. N., Luhur, M. R., Badarudin, A., Amiri, A., Sadri, R., ... & Teng, K. H. (2015). A comprehensive review of thermo-physical properties and convective heat transfer to nanofluids. *Energy, 89*, 1065-1086.

Tarokh, A., Mohamad, A., & Jiang, L. (2013). Simulation of conjugate heat transfer using the lattice Boltzmann method. *Numerical Heat Transfer, Part A: Applications, 63*(3), 159-178.

Tian, J., He, Z., Xu, T., Fang, X., & Zhang, Z. (2015). Rheological Property and Thermal Conductivity of Multi-walled Carbon Nanotubes-dispersed Non-Newtonian Nanofluids Based on an Aqueous Solution of Carboxymethyl Cellulose. *Experimental Heat Transfer* (in press).

Tsai, C., Chien, H., Ding, P., Chan, B., Luh, T., & Chen, P. (2004). Effect of structural character of gold nanoparticles in nanofluid on heat pipe thermal performance. *Materials Letters, 58*(9), 1461-1465.

Vafaei, S., & Wen, D. (2012). Convective heat transfer of aqueous alumina nanosuspensions in a horizontal mini-channel. *Heat and Mass Transfer, 48*(2), 349-357.

Verma, S. K., & Tiwari, A. K. (2015). Progress of nanofluid application in solar collectors: A review. *Energy Conversion and Management, 100*, 324-346.

Wang, J., Wang, M., & Li, Z. (2007). A lattice Boltzmann algorithm for fluid–solid conjugate heat transfer. *International Journal of Thermal Sciences, 46*(3), 228-234.

Yang, Y.-T., & Lai, F.-H. (2011). Numerical study of flow and heat transfer characteristics of alumina-water nanofluids in a microchannel using the lattice Boltzmann method. *International Communications in Heat and Mass Transfer, 38*(5), 607-614.

Zheng, L., Shi, B., Guo, Z., & Zheng, C. (2010). Lattice Boltzmann equation for axisymmetric thermal flows. *Computers and Fluids, 39*(6), 945-952.

Zhou, J. G. (2011). Axisymmetric lattice Boltzmann method revised. *Physical review E, 84*(3), 036704.

Zhou, M., Xia, G., Chai, L., Li, J., & Zhou, L. (2012). Analysis of flow and heat transfer characteristics of micro-pin fin heat sink using silver nanofluids. *Science China Technological Sciences, 55*(1), 155-162.

Zou, Q., & He, X. (1997). On pressure and velocity boundary conditions for the lattice Boltzmann BGK model. *Physics of Fluids (1994-present), 9*(6), 1591-1598.